Photodissociation and photodetachment of molecular negative ions. III. Ions formed in $CO_2/O_2/H_2O$ mixtures

P. C. Cosby, J. H. Ling, J. R. Peterson, and J. T. Moseley

Citation: The Journal of Chemical Physics **65**, 5267 (1976); doi: 10.1063/1.433026
View online: https://doi.org/10.1063/1.433026
View Table of Contents: http://aip.scitation.org/toc/jcp/65/12
Published by the American Institute of Physics

Photodissociation and photodetachment of molecular negative ions. III. Ions formed in $CO_2/O_2/H_2O$ mixtures*

P. C. Cosby, J. H. Ling, J. R. Peterson, and J. T. Moseley†

Molecular Physics Center, Stanford Research Institute, Menlo Park, California 94025
(Received 29 July 1976)

Total photodestruction cross sections for O_2^-, O_3^-, O_4^-, $O_2^-\cdot H_2O$, CO_4^-, CO_3^-, and $CO_3^-\cdot H_2O$ have been measured over the range from 6950 to 4579 Å (1.78–2.71 eV). In most cases the photodestruction of these ions can be attributed to specific photodissociation or photodetachment processes. The ions HCO_3^- and $HCO_3^-\cdot H_2O$ have also been investigated, and upper limits determined for their total photodestruction. The experiments were performed using a drift tube mass spectrometer coupled with an argon ion laser and a tunable dye laser. The cross section values vary from 2×10^{-20} to 1×10^{-17} cm^2, and in most cases photodissociation is the predominant process. In CO_3^- and O_3^- evidence is found for bound, predissociating excited states.

I. INTRODUCTION

In recent work[1–4] it was discovered that several ions important in the 60–90 km *D* region of the ionosphere undergo substantial photodissociation by visible light. Calculations[5] have shown that photodissociation is an important daytime loss mechanism for CO_3^- and $CO_3^-\cdot H_2O$ and could account for the rapid increase of electron density[6] in the *D* region at sunrise. Photodetachment and photodissociation processes are also important in gas discharge[7] and *e*-beam pumped[8] lasers, in magnetohydrodynamic generators[9], and in the study of photon-induced chemical reactions. In addition, there is fundamental interest in the interactions of photons with molecular ions. Studies of such interactions can provide information[10–15] about the location, shape and symmetry of the ground and excited states of ions, molecular bond energies, the electron affinity of the neutral parent, and energy partioning in photodissociation reactions.

In this paper we report total photodestruction cross sections over the range from 4579 to 6950 Å for a number of ions formed in mixtures of CO_2, O_2, and H_2O. The ions studied were chosen primarily for their possible importance in the *D* region, but the cross sections reported should also be useful in other applications. We make no attempt here at a detailed analysis of the results in terms of the structural properties of the ions, since each such analysis is quite involved and requires other experimental information in addition to the reported cross sections. In the cases of O_3^- and CO_3^-, however, such analysis is under way and is mentioned below.

II. APPARATUS AND TECHNIQUE

The experimental apparatus, which consists of a drift tube mass spectrometer, an argon ion laser, and a tunable dye laser, has been previously described[2,4] in some detail. Briefly, the negative ions are formed in the gas phase (0.050–0.400 torr) by electron attachment processes and subsequent ion–molecule reactions, and drift under the influence of a weak applied electric field through the background gas toward an extraction aperture. In these experiments, the ratio of the electric field to the neutral-gas density, E/N, is chosen such that the directed drift velocity is only about one tenth the mean thermal speed of the ions and gas molecules at room temperature. The drift distance is chosen so that the ions experience many thermalizing collisions following their production. Just before passing through the extraction aperture, the ions intersect the intracavity photons of the laser, which is chopped at 100 Hz. The ions that pass through the extraction aperture into the high vacuum analysis region are mass selected by a quadrupole mass spectrometer and individually detected by an electron multiplier.

Photons at seven discrete energies between 2.34–2.71 eV are obtained using the lines of a commercial argon ion laser. Continuously tunable photon energies between 1.78–2.43 eV are obtained using a commercial "jet-stream" dye laser pumped by the argon laser. In both cases, the drift tube is contained in the cavity of the appropriate laser. A major improvement over the earlier experiments has been achieved by using a more powerful commercial argon ion laser, having a nominal output power of 12 W (all lines) to pump the dye laser. Table I shows the dyes used, together with the wavelength range and peak intracavity powers obtained.

The wavelength of the dye laser is calibrated with a reversion spectroscope and a 0.3 m monochromator relative to the He–Ne and argon laser lines, to an accuracy of ±1 Å. In both laser configurations, the photon beam is linearly polarized perpendicular to the axis of the drift tube. The circulating power is sampled by calibrated low transmittance output couplers and monitored by a disk calorimeter.

Although, in principle, it is possible to determine absolute photodestruction cross sections in our experiment, all the cross sections reported here are put on an absolute scale by the following normalization procedure. The photodestruction cross section $\sigma(\lambda)$ for any negative ion A^- relative to the known cross section of another reference ion R^- is given by

$$\sigma_{A^-}(\lambda) = \sigma_{R^-}(\lambda)\frac{\ln(I_0/I)_{A^-}}{\ln(I_0/I)_{R^-}}\frac{P_{R^-}}{P_{A^-}}\frac{v_{A^-}}{v_{R^-}} \quad . \tag{1}$$

In this expression, I and I_0 are the numbers of ions detected at a given wavelength during the laser on and off periods, respectively, P_{R^-}/P_{A^-} is the ratio of the laser output powers measured during the accumulation of counts for each species, and v_{A^-}/v_{R^-} is the

TABLE I. Laser dyes.

Dye	Concentration[a]	Pump Lines[b]/Power(W)	Wavelength range (Å)	Cavity power (min/max, in W)	Lifetime[c] (h)
Cresyl violet[d,e]	0.001 *M* (EG) +0.0014 *M* R6*G* +0.1% COT +2% MEOH	All/16	7000–6500	19/51	5
Rhodamine *B*[e]	0.006 *M* (EG) +0.2% COT	All/16	6700–6000	42/187	24[f]
Rhodamine 6*G*[e]	0.003 *M* (EG) +0.2% COT +2% MEOH	All/16	6430–5650	40/220	Indefinite
Sodium fluorescein[e]	0.003 *M* (EG) +0.3% COT	All/16	5700–5275	17/120	Indefinite[f]
Coumarin 540[g]	0.0013 *M* (EG) +20% BA +0.2% COT	4880/8	5450–5125	13/54	36[f]

[a]Concentrations given in moles per liter (M) and percent by volume (%) for an ethylene glycol (EG) solution. R6G = rhodamine 6G dye; COT = 1,3,5,7-cyclooctatetraene; MEOH = methanol; BA = benzyl alcohol.
[b]Lines of the argon ion laser used to pump the dye.
[c]Lasing period of a 1.5 l solution of the dye over which the cavity power decreased by approximately 60%.
[d]The acetate, nitrate, and perchlorate salts of this dye have been used and are essentially equivalent in performance.
[e]Available from Eastman Kodak Co.
[f]COT must be frequently replenished to maintain performance.
[g]Equivalent to Coumarin 6. Available from Exciton Chemical Co.

ratio of mean speeds for each species when passing through the photon beam. This procedure avoids the necessity of knowing precisely the intracavity photon flux and the overlap integral between the ions and photons, both difficult quantities to determine experimentally. In many cases, the ratio v_A/v_R can also be determined much more accurately than can either of the velocities separately. A full discussion of these problems is found in Refs. 2 and 4. The absolute values of the cross sections reported here are based on a normalization to the O^- photodetachment cross section, as measured by Branscomb, Smith, and Tisone.[16]

The total photodestruction cross section in Eq. (1) describes the loss of an ion due to photodetachment or photodissociation (or both). Other mechanisms such as multiphoton processes, collisional dissociation, or reactions following photon excitation to a bound state are unlikely under our operating conditions, and we have not yet observed any such processes. Photodissociation may be observed directly by tuning the quadrupole mass filter to the mass of a photofragment ion and observing the increase in this ion when the laser is on,[1-3] or by using the difference between the mobilities of the parent and photofragment ions.[4] Photodetachment cannot be observed directly, but its presence can be inferred from differences in the photodestruction cross section and the apparent dissociation cross section obtained from observation of photofragment ions.

A particular feature of these experiments is the ability to bring the ions, that may be created in high vibrational or even excited electronic states, into thermal equilibrium with the background gas at essentially room temperature. One would expect strong effects from vibrational excitation on the photodissociation of an ion, and we have observed effects[1-4] attributed to such excitation. Due to the relatively high pressure and long drift distance of this apparatus, the ions can be made to undergo many thermalizing collisions, typically between 10^3–10^4, before the photon interaction. Often, changes in the total cross section are observed when the number of collisions is small, or when the drift velocity is larger than thermal velocity.

All results reported here were obtained under conditions such that the cross sections remained constant as the number of collisions was further increased, and all were obtained for drift velocities much less than thermal velocity. In many cases, extensive tests were made, such as those reported in Refs. 1–4, in a further attempt to detect effects of possible vibrational excitation. Therefore, except where specifically noted in the text, it is reasonable to assume that the cross sections reported here refer to a room temperature thermal distribution of vibrational levels in the parent ion. This situation differs significantly from photodissociation measurements made using fast ion beams,[11,14] where substantial vibrational excitation of the parent is observed, and where this excitation is encouraged to allow measurement of the vibrational spacings and populations in the ground state of the parent ion.

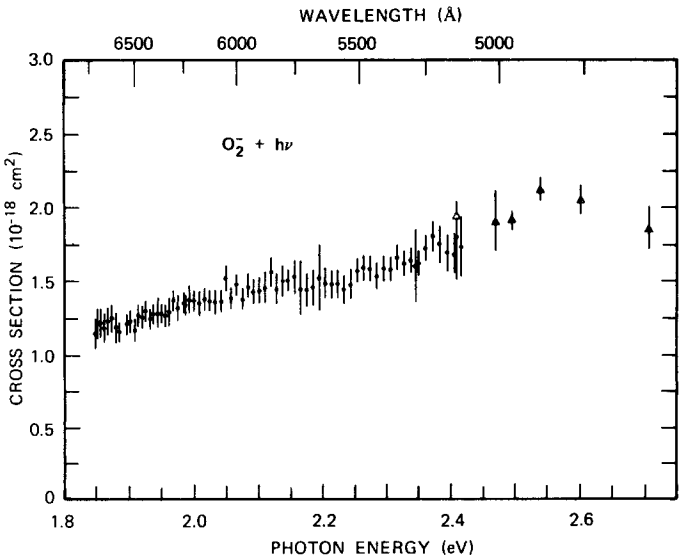

FIG. 1. Photodetachment cross section of O_2^- as a function of photon energy. The isolated error bars are the dye laser data; the triangles are data obtained at discrete argon ion laser lines.

III. PHOTODETACHMENT OF O_2^-

The O_2^- ions used for these measurements were produced in pure O_2 gas at a pressure of 0.1 torr, primarily by the three-body attachment reaction

$$e^- + O_2 + O_2 \rightarrow O_2^- + O_2 \ . \tag{2}$$

The measurements were made using a drift distance of at least 10.2 cm and an E/N of 10 Td (1 townsend = 10^{-17} V cm^2). Under these conditions only O^- and O_2^- ions were observed in significant concentrations. Small amounts of O_3^- and CO_3^-, less than 1 part in 10^3 of the O^- and O_2^- intensities, could also be observed.

Earlier measurements[4] on the photodetachment of O_2^- have been extended to cover a much wider wavelength range. The results are shown in Fig. 1 as a function of photon energy. The photodestruction here is clearly photodetachment, since the bond energy of O_2^- is greater 4 eV. The present results differ slightly from the earlier ones, between 6400–5650 Å but agree within the combined uncertainties. The present results show a smoother cross section with less possibility of the structure that was suggested earlier.[4] The absolute values are in excellent agreement with the measurements of Burch, Smith, and Branscomb,[17] who used a fast ion beam and color filters to select photon energies with a bandwidth of approximately 0.2 eV; with those of Warneck,[18] who also used a fast ion beam, but with a monochromator to obtain a photon energy resolution of 0.07 eV; and with very recent measurements of Vanderhoff and Beyer,[19] who used the discrete lines from argon and krypton lasers and a drift tube mass spectrometer technique similar to the one used here. The photon energy resolution in the present experiment is about 0.0003 eV.

The error bars given in Fig. 1 represent the root-mean-square sum of the statistical uncertainties in the measurement of $\ln(I_0/I)$ and the relative power terms in Eq. (1). Contributions to the uncertainty in the absolute scale consist of a 10% uncertainty in the value of the O^- photodetachment cross section, and a 4% uncertainty in the velocity ratio. Consequently, the absolute scale is considered accurate to ±12%.

IV. PHOTODISSOCIATION OF O_3^-

The O_3^- ions used in this study were produced in pure O_2 gas at pressures ranging from 0.2 to 0.4 torr, E/N of 10 Td, and drift distances of at least 10.2 cm, by the reaction[20–22]

$$O^- + 2O_2 \rightarrow O_3^- + O_2 \ . \tag{3}$$

As has been discussed,[4] it is energetically possible for O_3^- to photodetach and to photodissociate via the reaction

$$O_3^- + h\nu \rightarrow O^- + O_2 \tag{4}$$

at the photon energies used here.

The results of the total photodestruction measurements of O_3^- are given in Fig. 2 as a function of photon energy. As discussed in Ref. 4, comparison of the loss of O_3^- with the appearance of O^- photofragment ions indicates that (85% ± 15%) of the observed photodestruction occurs by the photodissociation process of Eq. (4). In addition, the measurements of the photodetachment cross section of O_3^- by Wong, Vorburger, and Woo[23] indicate that photodetachment contributes less than 10% to the total photodestruction shown in Fig. 2 at photon energies above 2.1 eV. To avoid the difficulties associated with normalizing the O_3^- cross section to O^-, when the O^- is not only destroyed by photodetachment but also produced in the photodissociation of O_3^-, the cross sections were normalized to those of O_2^- reported in the preceding section. The error bars in Fig. 2 were calculated as for O_2^-, but include the additional uncertainty in the O_2^- cross section. The uncertainty in the absolute scale is again ±12%.

This cross section shows a series of broad peaks and some subsidiary structures. Several researchers[24–27] have observed an absorption in O_3^- trapped in different solid environments in this wavelength range, with the absorption peaks spaced similarly to the observed broad peaks in the photodestruction cross section. Similar peaks have also been observed in the relative photodestruction measurements of O_3^- by Sinnott and Beaty.[28] We have previously discussed briefly[4] the possible interpretation of our earlier results on O_3^-. These new results will allow a more detailed analysis of this process and of the electronic states of O_3^-. The results of this investigation will be reported separately.

V. PHOTODESTRUCTION OF O_4^-

The O_4^- ions used in this study were produced in pure O_2 gas at pressures ranging from 0.3 to 0.4 torr, an E/N of 10 Td, and drift distances of at least 10.2 cm. The O_4^- ions are formed in the reaction

$$O_2^- + O_2 + O_2 \rightleftharpoons O_4^- + O_2 \ , \tag{5}$$

for which the forward and reverse rate constants have

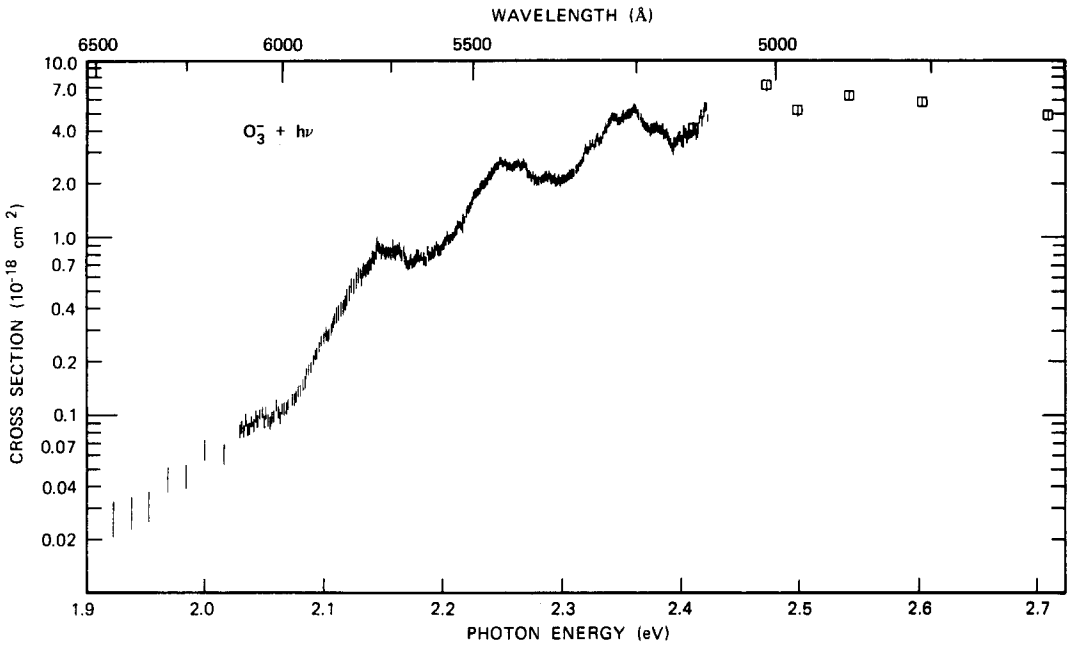

FIG. 2. Photodestruction cross section of O_3^- as a function of photon energy. The isolated error bars are the dye laser data; the squares are data obtained at discrete argon ion laser lines.

been measured[21,22] to be $4-5.1\times10^{-31}$ cm^6 sec^{-1} and $1.6-2.7\times10^{-14}$ cm^3 sec^{-1}, respectively. Thus, at the gas densities used here ($1.0-1.3\times10^{16}$ cm^{-3}), O_4^- ions are formed continuously along the drift path between the source and the laser beam. It should, therefore, not be assumed that these ions are in thermal equilibrium with the gas. However, the observed photodestruction cross section for O_4^- was found to be independent of variations in drift distance from 5.1 to 25.4 cm, and of variations in pressures from 0.3 to 0.4 torr, indicating either that the cross section may be insensitive to the internal energy of the O_4^- or that any internal excitation produced in the formation of O_4^- is rapidly quenched.

Total photodestruction cross sections for O_4^- are given in Fig. 3 as a function of photon energy. These cross sections were put on an absolute scale by normalization to the O_2^- cross sections of Fig. 1. The large number of O_3^- ions always present under the conditions used to form O_4^- prevents direct normalization to O^-. Of course, O_4^- might also photodissociate, yielding O_2^-, since the heat of formation of O_4^- is only 0.6 eV.[29] However, the effect of this process on the normalization would be negligible since the concentration of source-produced O_2^- in the photon interaction region is two orders of magnitude greater than that of O_4^-. The error bars in Fig. 3 again represent the statistical uncertainties, plus the relative uncertainty of the O_2^- cross section used for normalization. The uncertainty in the absolute scale is ±15%, including the uncertainty in the absolute O_2^- cross sections and in the velocity ratio.

Energetically, O_4^- may photodissociate and photodetach. Efforts to observe the production of photofragment ions were unsuccessful because of the large number of O^-, O_2^-, and O_3^- ions in the photon interaction region, compared with O_4^-, and because of the similar drift velocities[30] of the O_2^-, O_3^-, and O_4^- ions. The strong similarity between the O_4^- photodestruction cross section and the O_2^- photodetachment cross section is noted; the two are in fact equal within their mutual uncertainties at energies above 2.0 eV. The photodestruction mechanism for this ion can be determined by using substantially higher pressures to increase the relative O_4^- population or by conducting a beam experiment[11,14] and would probably help greatly in understanding the nature of the $O_2 \cdot O_2^-$ bonding in this ion. In any case, photodestruction must result in dissociation, since O_4 is not stable.

VI. PHOTODESTRUCTION OF $O_2^- \cdot H_2O$

The $O_2^- \cdot H_2O$ ions were formed by the reaction[21,22]

$$O_2^- + H_2O + M \rightarrow O_2^- \cdot H_2O + M\,, \qquad (6)$$

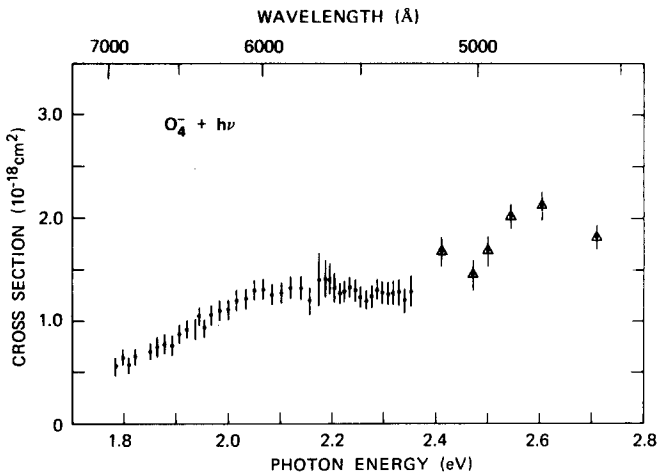

FIG. 3. Photodestruction cross section of O_4^- as a function of photon energy. The isolated error bars are the dye laser data; the triangles are data obtained at discrete argon ion laser lines.

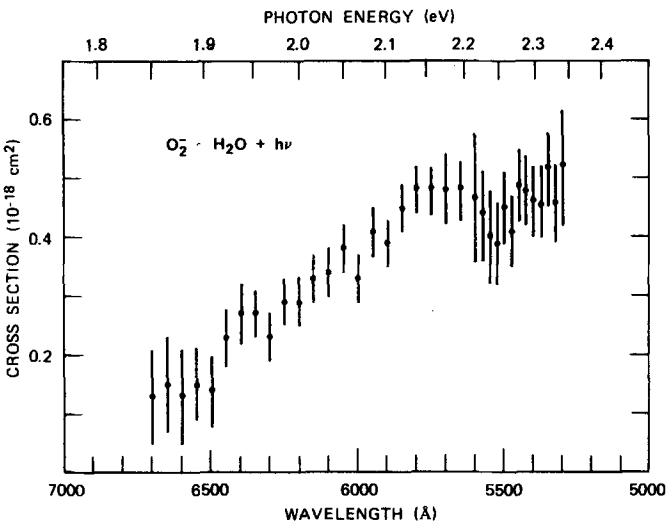

FIG. 4. Photodestruction cross section of $O_2^- \cdot H_2O$ as a function of photon wavelength.

in a 98 : 2 mixture of O_2 and H_2O at a total pressure of 0.1 torr, an E/N of 10 Td, and drift distances of at least 10.2 cm. The results are presented in Fig. 4 as a function of wavelength. The uncertainties were determined as for O_4^-, and the uncertainty in the absolute scale is again ±15%. Also, as in the O_4^- case, it is not asserted that the $O_2^- \cdot H_2O$ ions were in thermal equilibrium with the gas when they passed through the laser beam; nor was the photodestruction channel determined. Again, both photodetachment and photodissociation are energetically possible, and photodetachment will yield dissociation into O_2, H_2O, and an electron.

VII. PHOTODISSOCIATION OF CO_3^-

The CO_3^- ions used in this study were formed in pure CO_2 gas, and in mixtures of O_2 and CO_2, at a pressure of 0.050 torr, an E/N of 10 Td, and a drift distance of at least 10.2 cm. The formation, equilibration, and photodestruction processes have been extensively discussed[1-3] and will not be repeated here. It is concluded that the results, presented in Fig. 5, are for the photodissociation of CO_3^-, which is in thermal equilibrium at room temperature, by the process

$$CO_3^- + h\nu \rightarrow O^- + CO_2 \,. \tag{7}$$

The absolute scale was determined by normalization to both O^- and O_2^- and has an uncertainty of ±15%.

We have noted[3] that the structure in this cross section reflects the vibrational levels of a bound, predissociating state of CO_3^-. We have recently made a detailed analysis[31] of the CO_3^- spectrum, and summarize the results here for completeness. The bond energy $D(CO_2\text{–}O^-)$ is (1.8 ± 0.1) eV, and the electron affinity E. A. (CO_3) is (2.9 ± 0.3) eV. Assuming the ground state of CO_3^- is $^2B_2$, the excited state responsible for the observed structure is $^2A_1$. The three bending modes of this state have frequencies of 990, 1470, and 880 cm^{-1}, and the ground level of this state is 1.520 eV above the ground level of the ground state.

VIII. PHOTODISSOCIATION OF $CO_3^- \cdot H_2O$

The $CO_3^- \cdot H_2O$ ions were formed using two different gas mixtures. A mixture of CO_2 and H_2O at 0.05 torr, with a H_2O concentration of less than 1% (by volume), at an E/N of 10 Td and a drift distance of 5.1 cm or greater, produced the ions O^-, CO_3^-, $CO_3^- \cdot H_2O$, OH^-, HCO_3^-, and $HCO_3^- \cdot H_2O$. Higher hydrates of CO_3^- and HCO_3^- could be observed only at significantly higher H_2O concentrations (>10%). A mixture of O_2, CO_2, and H_2O was also used in this work. The concentration of CO_2 was maintained at approximately 5%, while that of H_2O was less than 1%. At an E/N of 5 or 10 Td, a drift distance of 20.3 cm, and a total pressure of 0.1 or 0.15 torr, O_2^- and traces of $O_2^- \cdot H_2O$ were formed in addition to those ions observed in the CO_2–H_2O mixture.

The $CO_3^- \cdot H_2O$ is formed in the three-body reaction[32]

$$CO_3^- + H_2O + M \rightarrow CO_3^- \cdot H_2O + M \,. \tag{8}$$

Observations of the arrival time spectra of the ions when the source was pulsed and of the photodestruction behavior of each of the ions revealed no evidence of ion–molecule reactions or of photon interactions coupling the ions based on O^- (CO_3^- and its hydrates) and those based on OH^- (HCO_3^- and its hydrates). In the CO_2–H_2O mixture, the total photodestruction cross section for $CO_3^- \cdot H_2O$ could be measured relative to the CO_3^- cross section with negligible interference[2] from other photodestruction processes when proper account was taken of photofragment CO_3^- ions. In the O_2–CO_2–H_2O mixtures, the $CO_3^- \cdot H_2O$ cross section could be mea-

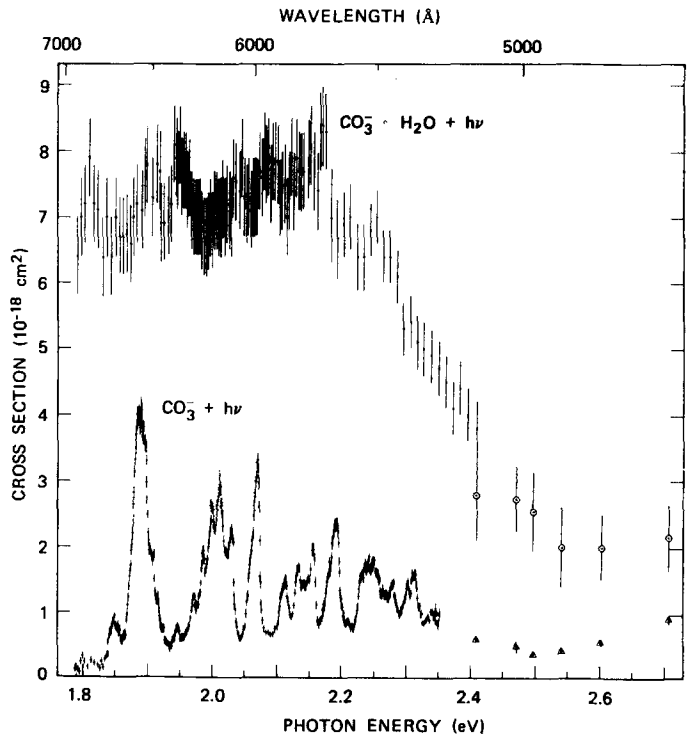

FIG. 5. Total photodestruction cross sections of CO_3^- (lower) and $CO_3^- \cdot H_2O$ (upper) as a function of photon energy. The open triangles and open circles are data obtained at discrete argon ion laser lines for CO_3^- and $CO_3^- \cdot H_2O$, respectively; the isolated error bars are the dye laser data.

sured relative to that of O_2^- with no measurable interference of photofragment ions.

The results of the $CO_3^- \cdot H_2O$ photodestruction measurements are given in Fig. 5. The error bars include the statistical uncertainties in $\ln(I_0/I)$, in the relative power measurement, and in the CO_3^- and O_2^- cross sections used for normalization. The uncertainty in the absolute scale is ± 20%, reflecting the absolute uncertainties in the CO_3^- and O_2^- cross sections and in the ratios of the relative velocities of these ions to that of $CO_3^- \cdot H_2O$.

Since the electron affinity of CO_3 is (2.9 ± 0.3) eV and the electron attachment energy of $CO_3^- \cdot H_2O$ will exceed that of CO_3^- by approximately the $CO_3^- \cdot H_2O$ bond energy (~0.5 eV), the observed photodestruction of $CO_3^- \cdot H_2O$ must be photodissociation.

Dissociation into $CO_3^- + H_2O$ and $O^- \cdot H_2O + CO_2$ should be energetically permitted over the entire wavelength range used here. In addition, the threshold for dissociation into $O^- + CO_2 + H_2O$ would be expected at 5500 Å or shorter wavelengths, given the bond energies involved.

We have searched for the production of these photofragment ions at wavelengths between 5145–6400 Å. In this region only CO_3^- photofragments were observed, and in amounts that accounted for 90% ± 10% of the total $CO_3^- \cdot H_2O$ photodestruction. No evidence was observed for the production of O^- or $O^- \cdot H_2O$ photofragments by the hydrate. However, it is known[32] that the $O^- \cdot H_2O$ ion reacts rapidly ($k > 1 \times 10^{-11}$ cm^3/sec) in oxygen gas, and it is likely that a similar reaction will take place in CO_2 at about the same or even faster rate. For the drift tube conditions used here, more than half (and possibly all) of any photofragment $O^- \cdot H_2O$ would consequently be destroyed by reaction prior to their detection. It is similarly difficult to assess the possible production of photofragment O^- from $CO_3^- \cdot H_2O$. For the drift tube conditions used here, the maximum number of photofragment O^- ions that could possibly be produced from the hydrate (i.e., ≤20% of the total $CO_3^- \cdot H_2O$ photodestruction) would be two orders of magnitude smaller than the number of photofragment O^- ions that are simultaneously produced from CO_3^-. Moreover, the nearly identical mobilities of CO_3^- and $CO_2^- \cdot H_2O$ do not permit resolution of their respective photofragments using time-of-flight techniques. We therefore conclude that although photodissociation of $CO_3^- \cdot H_2O$ to form either O^- or $O^- \cdot H_2O$ photofragments cannot be entirely ruled out, the predominant photodissociation channel at visible wavelengths yields $CO_3^- + H_2O$.

We have previously[2] discussed several possible interpretations of the $CO_3^- \cdot H_2O$ photodestruction at the argon laser lines. The cross section obtained using the dye laser and our interpretation of the CO_3^- results[31] now allow a better understanding of the $CO_3^- \cdot H_2O$ photodissociation. We have concluded that CO_3^- absorbs at photon energies between 1.52–2.35 eV into a state that is predissociative above 1.8 eV. Above 2.35 eV, CO_3^- continues to absorb, although less strongly, probably into one or more other predissociating states. Between 1.8–2.35 eV, only three modes of CO_3^-, identified as bending modes, are found to predissociate, but it is likely that absorption also occurs into both the symmetric and antisymmetric stretch modes of the excited electronic state. If the weak $CO_3^- - H_2O$ bond (~0.5 eV)[32] is primarily electrostatic, the presence of the H_2O should only slightly perturb the electronic states of the isolated CO_3^- ion. Thus, photoabsorption by the hydrate should take place over essentially the same range of photon energies as for CO_3^-. But when the cluster absorbs, in addition to radiation back to the ground state or dissociation into O^- or $O^- \cdot H_2O$, it has a lower energy channel for disposing the energy acquired in the photoabsorption—ejection of the H_2O.

It is seen in Fig. 5 that the similarity in the energy dependences of the mean destruction cross section for the CO_3^- and $CO_3^- \cdot H_2O$ ions at photon energies above approximately 1.9 eV supports this model, as does the fact that $CO_3^- \cdot H_2O$ continues to dissociate at energies below the photodissociation threshold of the CO_3^-. It is therefore expected that the threshold for the hydrate photodissociation will occur in the region of the predicted origin of the 1^2A_1 state of CO_3^- at 1.52 eV. The actual threshold will depend on the relative interactions of the H_2O with the ground and excited CO_3^- states. It is not now understood how the photoexcited levels in the region of 1.8 eV, which are only about 0.3 eV above the ground level of the 1^2A_1 state of CO_3^-, are effective in supplying the ≃0.5 eV required to dissociate the H_2O cluster. Certainly there is sufficient electronic energy, and it may be that radiationless transitions to vibrationally excited levels of the ground electronic state occur, which are then partly internally relaxed by dissociation into $CO_3^- + H_2O$.

The fact that the photodissociation cross section for $CO_3^- \cdot H_2O$ is substantially greater than that for CO_3^- can be explained if it is easier for the excited complex to localize 0.5 eV for ejection of the H_2O than for CO_3^- to localize 1.8 eV for the ejection of O^-. Thus the predissociation channel can compete more effectively with the radiation (fluorescence) channel in the hydrate than in the parent.

The fact that the $CO_3^- \cdot H_2O$ destruction cross section does not exhibit the same detailed structure as CO_3^- may result from additional vibrational modes that are excited by absorption but which do not contribute to dissociation in CO_3^- itself. It may also be expected that the CO_3^- absorption frequencies in the hydrate are slightly dependent on the orientation of the water molecule and that the vibrational excitation present in the $CO_3^- \cdot H_2O$ bound at 300 °K thus causes absorption spectrum of the hydrated CO_3^- to be smoothed out compared with that of CO_3^-.

The presence of the water molecule (and its associated electric dipole field) may also increase the CO_3^- absorption cross section, thus accounting for the three times larger destruction cross section in the hydrate. Since it is unlikely that changes in the Franck–Condon factors alone could lead to such an increase, this effect would require a change in the oscillator strengths of the transitions. In view of the close similarity of

TABLE II. Total photodestruction cross section of CO_4^-.

Wavelength (Å)	Cross section (10^{-20} cm^2)
6900	< 3.0
6500	< 1.6
6400	< 2.0
6200	< 2.0
6000	< 2.1
5800	< 2.8
5500	< 2.0
5200	2.5 ± 2.3
5145	3.7 ± 2.0

the envelopes of the two cross sections, indicating that the absorbing levels of the hydrate are essentially those of the isolated CO_3^-, this explanation is not very convincing.

While this discussion is clearly not definitive, the present results do allow a narrowing of the alternatives proposed earlier[2] and suggest additional experiments that should assist in our understanding of $CO_3^- \cdot H_2O$ and its photodestruction characteristics.

IX. PHOTODESTRUCTION OF HCO_3^- AND $HCO_3^- \cdot H_2O$

As mentioned in the preceding section, addition of H_2O to CO_2 in the drift tube results in the production of OH^-, HCO_3^-, and hydrates of HCO_3^-. Alternatively, the HCO_3^- ion can be produced[32] in the absence of hydrates by using a 98 : 2 mixture of CO_2 and CH_4. We have investigated the total photodestruction cross section of HCO_3^- by each method of formation, using the tunable dye laser at wavelengths between 6500–5145 Å. We found that the cross section for this ion is less than 3×10^{-20} cm^2 over this wavelength range, and possibly zero.

Results for $HCO_3^- \cdot H_2O$ were similar to those for HCO_3^-. The total photodestruction cross section was observed to be less than 7×10^{-21} cm^2 at 5145 Å, and statistically consistent with zero over the range from 6500–4579 Å.

We have previously reported[2] small but nonzero photodestruction cross sections for HCO_3^- at four argon ion wavelengths. However, in the course of our further work using the drift tube, we found that the photon beam produced a small modulation (< 0.1%) of the detected current of a nonabsorbing ion species when it was in the presence of relatively high densities of other species that have large photodestruction cross sections. We believe that this modulation results from the large changes in ion density that occur in the photon interaction region when significant fractions of the absorbing ions in this region are photodetached. This effect can be identified by monitoring the apparent photodestruction cross section as a function of total ion density. The modulation is found to occur for HCO_3^- at the dye laser wavelengths because of the high relative densities of O^- and OH^- ions present in both the CO_2–H_2O and CO_2–CH_4 mixtures. The total photodestruction cross sections reported here were obtained at a sufficiently low ion density that the modulation effect was undetectable. This precaution was not taken when the cross sections were measured at the argon ion laser wavelengths. Consequently, those values[2] should be considered only as upper limits to the HCO_3^- total photodestruction cross section, until the cross section at the argon ion laser wavelengths can be investigated as a function of total ion density.

X. PHOTODESTRUCTION OF CO_4^-

The CO_4^- studied here was formed[32] in a 95 : 5 mixture of O_2 and CO_2 at a pressure of 0.1 torr, an E/N of 5 Td, and a drift distance of 30.5 cm. This ion has an electron affinity[33] of 1.22 eV and a CO_2–O_2^- bond energy[33] of 0.8 eV. It therefore is energetically possible for it to both photodissociate and photodetach at these photon energies. The total photodestruction cross section of CO_4^- was measured at wavelengths between 6900–5145 Å, using the tunable dye laser, and at 5145 Å, using the argon ion laser.

The results, summarized in Table II, show that the cross section is less than 3×10^{-20} cm^2 at wavelengths between 6900–5500 Å. However, small but nonzero cross sections are measured at 5200 and 5145 Å. Because of the small size of these cross sections and the low abundance of CO_4^- produced in the drift tube, possible photofragments of CO_4^- could not be observed. Thus it is not known whether the photodestruction of this ion is due to photodetachment or to photodissociation.

XI. SUMMARY AND CONCLUSIONS

Photon interactions with nine molecular negative ions have been studied over the wavelength range from 6950 to 4579 Å. For three of these ions, O_3^-, CO_3^-, and $CO_3^- \cdot H_2O$, photodissociation into an ionic photofragment was observed, and evidence was obtained for the existence of bound, predissociative states in these species. For three ions, O_4^-, $O_2^- \cdot H_2O$, and CO_4^-, photodestruction was observed, which probably results in dissociation, but it was not determined whether photofragment ions were produced or neutral products and an electron. One ion, O_2^-, which can only photodetach at these wavelengths, yielded absolute values in agreement with earlier work. Two ions, HCO_3^- and $HCO_3^- \cdot H_2O$, apparently neither photodetach or photodissociate over this wavelength range.

The initial motivation for these studies was the importance of these ions in the ionosphere. However, it is apparent that these measurements provide valuable information for studies of ionic structure and potential surfaces. Such a study has been done[28] for CO_3^-, and one is under way for O_3^-. Application of ion photofragment energy spectroscopy[11,14] to ions such as CO_3^- and O_3^- should further extend our knowledge of their structure and dissociation mechanisms.

*This research was supported by the U. S. Army Ballistics Research Laboratories through the U. S. Army Research Office.

†Address for 1975–76 academic year: Laboratoire des Collisions Ioniques, Université de Paris-Sud, 91405 Orsay, France.
[1]J. T. Moseley, R. A. Bennett, and J. R. Peterson, Chem. Phys. Lett. **26**, 288 (1974).
[2]J. T. Moseley, P. C. Cosby, R. A. Bennett, and J. R. Peterson, J. Chem. Phys. **62**, 4826 (1975).
[3]P. C. Cosby and J. T. Moseley, Phys. Rev. Lett. **34**, 1603 (1975).
[4]P. C. Cosby, R. A. Bennett, J. R. Peterson, J. T. Moseley, J. Chem. Phys. **63**, 1612 (1975).
[5]J. R. Peterson, J. Geophys. Res. **81**, 1433 (1976).
[6]R. P. Turco and C. F. Sechrist, Radio Sci. **7**, 717 (1972); R. P. Turco, *ibid.* **9**, 655 (1974).
[7]W. L. Nighan and W. J. Wiegand, Phys. Rev. A **10**, 922 (1974).
[8]D. L. Huestis *et al.*, *"Visible Absorption by Rare Gas Molecular Ions and Excimers,"* Paper RN4, 31st Symposium on Molecular Structure and Spectroscopy, Ohio State University, 1976.
[9]F. E. Spencer, J. C. Hendrie, and D. Bienstock, Paper VIII 4, 13th Symposium on Engineering Aspects of Magnetohydrodynamics, Stanford University, 1973.
[10]G. H. Dunn, Phys. Rev. **172**, 1 (1968).
[11]N. P. F. B. van Asselt, J. G. Mass, and J. Los, Chem. Phys. Lett. **24**, 555 (1974); Chem. Phys. **5**, 429 (1974); **11**, 253 (1975).
[12]G. E. Busch and K. R. Wilson, J. Chem. Phys. **56**, 3638 (1972).
[13]R. N. Zare, Ph. D. thesis, Harvard University, 1964; Mol. Photochem. **4**, 1 (1972).
[14]J. B. Ozenne, D. Pham and J. Durup, Chem. Phys. Lett. **17**, 422 (1972); J. B. Ozenne, J. Durup, R. W. Odom, C. Pernot, A. Tabche-Fouhaille, and M. Tadjeddine, Chem. Phys. **16**, 75 (1976).
[15]G. E. Busch and K. R. Wilson, J. Chem. Phys. **56**, 3626 (1972).
[16]L. M. Branscomb, S. J. Smith, and G. Tisone, J. Chem. Phys. **43**, 2906 (1965).
[17]D. S. Burch, S. J. Smith, and L. M. Branscomb, Phys. Rev. **112**, 171 (1958).
[18]P. Warneck, Laboratory Measurements of Photodetachment Cross Sections of Selected Negative Ions GCA Tech. Rept. 69-13-N, GCA Corp., Bedford, Massachusetts, 1969.
[19]J. A. Vanderhoff and R. A. Beyer, Bull. Am. Phys. Sec. **21**, 85 (1976); J. Chem. Phys. (in press).
[20]R. M. Snuggs, D. J. Volz, I. R. Gatland, J. M. Schummers, D. W. Martin, and E. W. McDaniel, Phys. Rev. A **3**, 487 (1971).
[21]J. L. Pack and A. V. Phelps, Bull. Am. Phys. Soc. **16**, 214 (1971).
[22]J. D. Payzant and P. Kebarle, J. Chem. Phys. **56**, 3482 (1972).
[23]S. F. Wong, T. V. Vorburger and S. B. Woo, Phys. Rev. A **5**, 2598 (1972).
[24]M. E. Jacox and D. E. Milligan, J. Mol. Spectry. **43**, 148 (1972); Chem. Phys. Lett. **14**, 518 (1972).
[25]P. A. Giguere and K. Herman, Can. J. Chem. **52**, 3941 (1974).
[26]J. B. Bates and J. C. Pigg, J. Chem. Phys. **62**, 4227 (1975).
[27]L. Andrews, J. Chem. Phys. **63**, 4465 (1975).
[28]G. Sinnott and E. C. Beaty, *Seventh International Conference on the Physics of Electronic and Atomic Collisions, Abstracts of Papers* (North Holland, Amsterdam, 1971), p. 176. Also E. C. Beaty (private communication).
[29]D. C. Conway and L. E. Nesbitt, J. Chem. Phys. **48**, 509 (1968).
[30]R. M. Snuggs, D. J. Volz, J. H. Schummers, D. W. Martin, and E. W. McDaniel, Phys. Rev. A **3**, 477 (1971).
[31]J. T. Moseley, P. C. Cosby, and J. R. Peterson, J. Chem. Phys. **65**, 2512 (1976).
[32]F. C. Fehsenfeld and E. E. Ferguson, J. Chem. Phys. **61**, 3181 (1974).
[33]J. L. Pack and A. V. Phelps, J. Chem. Phys. **45**, 4316 (1966).